Available online at www.sciencedirect.com
SCIENCE DIRECT®
Journal of Power Sources 138 (2004) 79–85
JOURNAL OF POWER SOURCES
www.elsevier.com/locate/jpowsour

Thermally nitrided stainless steels for polymer electrolyte membrane fuel cell bipolar plates Part 2: Beneficial modification of passive layer on AISI446

H. Wang[a], M.P. Brady[b], K.L. More[b], H.M. Meyer III[b], John A. Turner[a,*]

[a] *National Renewable Energy Laboratory, 1617 Cole Boulevard Golden, CO 80401-3393, USA*
[b] *Oak Ridge National Laboratory, Oak Ridge, TN 37831, USA*

Received 17 May 2004; accepted 8 June 2004
Available online 27 August 2004

Abstract

Thermal nitridation of AISI446 mod-1 superferritic stainless steel for 24 h at 1100 °C resulted in an adherent, inward growing surface layer based on $(Cr, Fe)_2N_{1-x}$ (x = 0–0.5). The layer was not continuous, and although it resulted in low interfacial contact resistance (ICR) and good corrosion resistance under simulated polymer electrolyte membrane fuel cell (PEMFC) cathodic conditions; poor corrosion resistance was observed under simulated anodic conditions. Nitridation for 2 h at 1100 °C resulted in little nitrogen uptake and a tinted surface. Analysis by SEM, XPS, and AES suggested a complex heterogeneous modification of the native passive oxide film by nitrogen rather than the desired microns-thick exclusive Cr-rich nitride layer. Surprisingly, this modification resulted in both good corrosion resistance under simulated cathodic and anodic conditions and low ICR, well over an order of magnitude lower than the untreated alloy. Further, little increase in ICR was observed under passivating polarization conditions. The potential of this phenomenon for PEMFC bipolar plates is discussed.

Keywords: Nitridation; Stainless steel; Ferrite; PEMFC; Bipolar plate

1. Introduction

Worldwide interest in the polymer electrolyte membrane fuel cell (PEMFC) is growing due to its clean chemical energy conversion characteristics and its conceptually simple design and operation [1]. The bipolar plate is a key component in a PEMFC, but current bipolar plate materials suffer from high costs, and lack of a viable mass-manufacturing pathway. Recently, it was discovered that thermally grown Cr nitrides (CrN/Cr_2N) on a model Cr-bearing alloy, Ni–50Cr (wt.%), show great promise in PEMFC bipolar plate environments [2–4]. This alloy is, however, too expensive for many PEMFC applications. In Part 1 of this paper [5], we applied similar thermal nitridation conditions to a relatively inexpensive, commercially available austenitic stainless steel, 349^{TM}. A discontinuous discrete mixture of CrN, Cr_2N and $(Cr, Fe)_2N_{1-x}$ (x = 0–0.5) phase surface particles overlying an exposed γ austenite based matrix, rather than a continuous nitride surface layer, was formed. This resulted in unacceptably high corrosion rates under simulated PEMFC anodic and cathodic conditions. Part 2 of this paper explores the nitridation behavior and corrosion resistance of a superferritic stainless steel, AISI446 mod 1. This alloy was selected because of its high level of Cr (27–28 wt.%), its promising performance in simulated PEMFC environments [6], and to survey the nitridation response of a ferritic stainless steel, as substrate alloy composition and structure can have a significant impact on the nature and morphology of the nitride products that form.

* Corresponding author. Tel.: +1 303 275 4270; fax: +1 303 275 3033.
E-mail address: john_turner@nrel.gov (J.A. Turner).

0378-7753/$ – see front matter © 2004 Elsevier B.V. All rights reserved.
doi:10.1016/j.jpowsour.2004.06.064

2. Experimental

2.1. Material

Stainless steels plates of AISI446 were provided by J&L Specialty Steel, Inc. The nominal composition is: 0.03 C, 28.37 Cr, 3.50 Mo, 2.96 Ni, 0.43 Mn, 0.42 Si, 0.75 Ti + Nb (wt.%) with Fe as the reminder. This composition is representative of the mod-1 variation of AISI446 (UNS S44660, referred to in the remainder of this paper as AISI446 for convenience). The analyzed composition of this alloy by inductively coupled plasma (ICP) and gas fusion was 0.02 C, 27 Cr, 3.7 Mo, 2 Ni, 0.37 Mn, 0.4 Si, 0.47 Ti, 0.03 Nb, 0.1 V, 0.1 Cu, 0.06 Co, 0.06 Al, 0.012 P, 0.0253 N, 0.001 S, 0.0025 O, balance Fe (wt.%). Alloy plates were cut into samples of 2.54 cm × 1.27 cm (1.0 in. × 0.5 in.). The samples were ground with #600 grit SiC abrasive paper, rinsed with acetone and dried with nitrogen gas.

Thermal nitridation was carried out in a high vacuum alumina furnace that was backfilled with pure nitrogen to 1 atm, the nitrogen flow stopped, and then the furnace was heated to 1100 °C. The baseline 2 h, 1100 °C nitridation treatment developed for the model Ni–50Cr alloy [2,3] resulted in nitrogen uptake on the order of only 0.5 mg cm^{-2} for the AISI446, and the sample appeared tinted (indicative of a very thin surface layer) rather than the usual opaque gray appearance associated with a thick (micron range) nitride surface layer. Therefore, an additional nitridation treatment with a hold time of 24 h at 1100 °C was also examined. This resulted in nitrogen uptake on the order of 4–5 mg cm^{-2} and the more typical uniform gray appearance.

2.2. Characterization

The thermally nitrided AISI446 was characterized by scanning electron microscopy (SEM), glancing angle X-ray diffraction (XRD), Auger electron spectroscopy (AES), X-ray photoelectron spectroscopy (XPS), and cross section transmission electron microscopy (TEM) using focused ion beam milling for specimen preparation. Polarization studies were conducted under simulated aggressive PEMFC environments using 1 M H_2SO_4 + 2 ppm F^- solution at 70 °C sparged either with air (PEMFC cathodic conditions) or with hydrogen gas (PEMFC anodic conditions). The potentials reported are relative to the saturated calomel electrode (SCE) unless otherwise noted. Interfacial contact resistance (ICR) measurements were carried out at room temperature with metallic, as-nitrided, and polarized AISI446 samples. Details for the ICR measurements were described elsewhere [7]. For the polarized AISI446 samples, potentiostatic polarization was conducted only on one face of the sample. ICR data for these samples is presented as a sum of *both* faces, polarized and as-nitrided. Details of the characterization techniques and testing protocol are provided in Part 1 of this paper [5].

3. Results and discussion

3.1. The 24 h nitrided AISI446

Potentiostatic polarization measurements for 24 h nitrided AISI446 in 1 M H_2SO_4 + 2 ppm F^- at 70 °C are shown in Fig. 1 for 0.6 V in air sparged solution (cathodic simulation, Fig. 1a) and for −0.1 V in hydrogen gas sparged solution (anodic simulation, Fig. 1b). Low current densities were observed under the simulated cathodic conditions, on the order of 2×10^{-6} A cm^{-2}. However, under the simulated anodic conditions, high current densities were obtained, which stabilized at about 0.8×10^{-3} A cm^{-2} over the course of a 5 h hold. Current densities on the order of 10^{-6} A cm^{-2} are considered sufficiently promising to move forward to fuel cell testing (see Part 1 of this paper for further details). The high current densities indicate that the 24 h nitrided material is not promising for PEMFC bipolar plate applications.

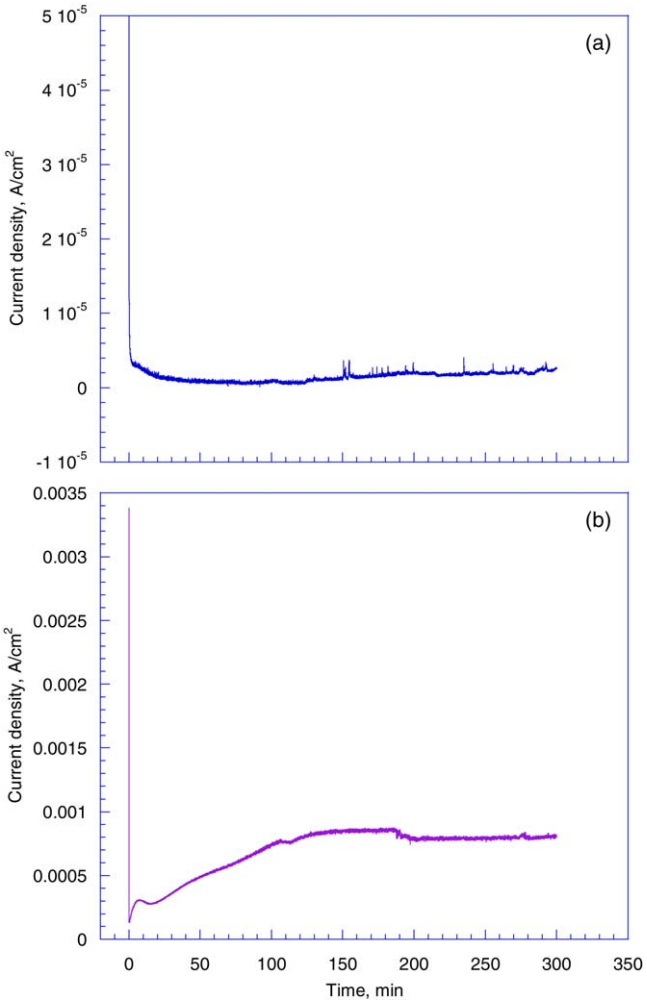

Fig. 1. Transient currents of 24 h nitrided AISI446 stainless steel in simulated PEMFC environments: (a) sample was polarized at 0.6 V and the solution was purged with air; (b) sample was polarized at −0.1 V and the solution was purged with hydrogen gas.

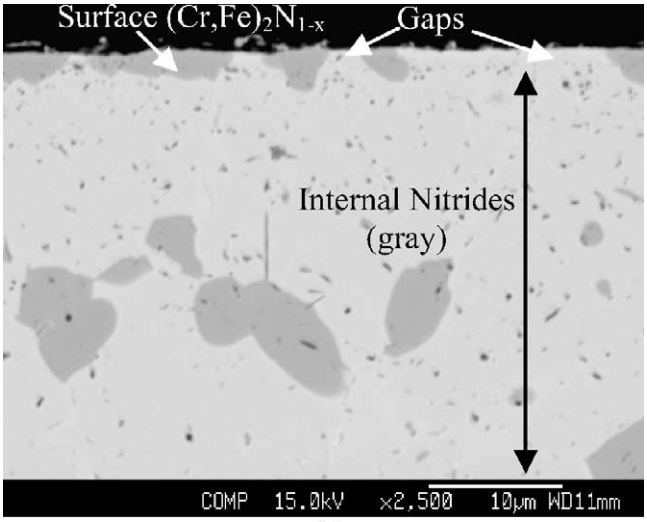

Fig. 2. SEM cross-section of 24 h nitrided AISI446 steels: (a) sample exposed in simulated PEMFC cathode environment; (b) sample exposed in simulated PEMFC anode environment.

SEM cross-sections of the polarized samples are shown in Fig. 2. The sample exposed in the PEMFC cathode environment (Fig. 2a) showed a similar microstructure to as-nitrided AISI446 material, and consisted of an inward growing Cr-rich nitride scale overlying an extensive zone of internal Cr-rich nitrides. XRD and EDS data indicate that the Cr-rich nitride external and internal phases were consistent with the $(Cr,Fe)_2N_{1-x}$ (x = 0–0.5) phase rather than with Cr_2N (although trace quantities of CrN were also detected). This microstructure is in contrast to that observed for nitrided 349^{TM} stainless steel [5], which showed isolated, loosely adherent discrete Cr_2N/$(Cr,Fe)_2N_{1-x}$ (x = 0–0.5)-based surface particles. However, unlike the inward growing Cr_2N layer formed on nitrided Ni–50Cr [5], the $(Cr,Fe)_2N_{1-x}$ (x = 0–0.5) layer formed on 24 h nitrided AISI446 was not continuous. It is interesting to note that this lack of continuity did not result in poor corrosion resistance under the simulated cathodic test conditions, but did result in very poor corrosion resistance under the simulated anodic conditions.

The microstructure of 24 h nitrided AISI446 following exposure to the simulated PEMFC anodic conditions is shown in Fig. 2b. Extensive dissolution and attack was evident at and along the $(Cr,Fe)_2N_{1-x}$/alloy interfaces, suggestive of a local galvanic couple effect. It is speculated that oxygen, which is available under cathodic conditions, allowed for local passivation and protection of the surface in these regions. However, under the hydrogen-purged anodic conditions, oxygen was not sufficiently available, or more likely, the mechanism of formation sufficiently altered, that a protective passive layer could not be locally established in the gap regions of $(Cr,Fe)_2N_{1-x}$ coverage.

3.2. The 2 h nitrided AISI446

Dynamic polarization of 2 h nitrided AISI446 steel in 1 M H_2SO_4 + 2 ppm F^- at 70 °C in air and hydrogen gas sparged solutions is shown in Fig. 3. The polarization curves are almost identical, indicating a minimal effect of the sparging gas. Polarization curves with fresh AISI446 steels in the same environments are plotted for comparison. With fresh AISI446 samples, the sparging gases have significant influence in the corrosion potential and the anodic polarization up to 0.2 V. At 0.2 V and above, their effect is negligible. With 2 h nitridation, the OCP shifts anodically. The corrosion potential of the 2 h nitrided 446 was at around −0.09 V in hydrogen-sparged solution and around −0.1 V in the air-sparged solution. This is very close to the expected anodic operating conditions in PEMFC's of −0.1 V, and could make it susceptible to dissolution. The changes in corrosion potential reflect that the surface condition of the 2 h nitrided AISI446 steel is clearly different

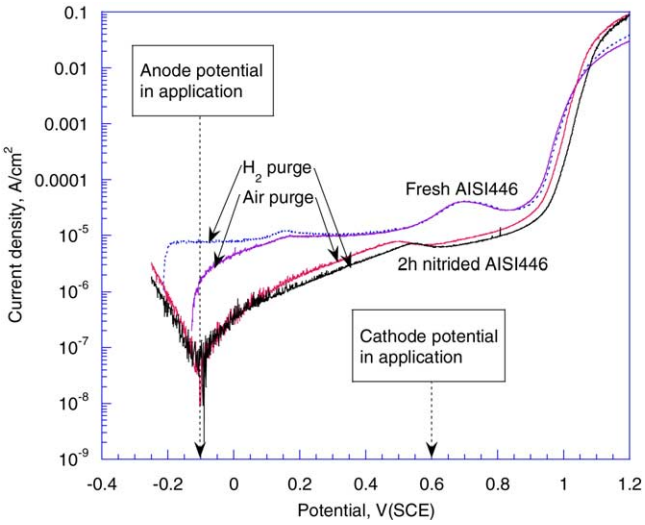

Fig. 3. Dynamic polarization behavior of 2 h nitrided AISI446 stainless steel in 1 M H_2SO_4 + 2 ppm F^- at 70 °C purged either with air or hydrogen gas. The anode and cathode potentials in PEMFC application are marked. Polarization curves with untreated (fresh) AISI446 are plotted for comparison.

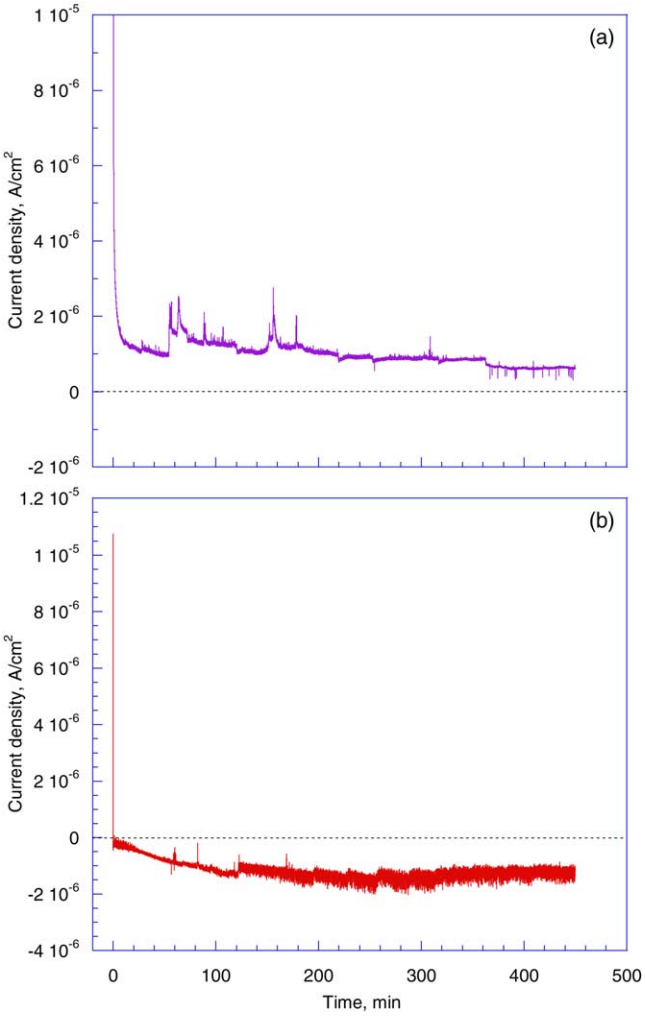

Fig. 4. Transient currents of 2 h nitrided 446 stainless steel in simulated PEMFC environment: (a) sample was polarized at 0.6 V and the solution was purged with air; (b) sample was polarized at −0.1 V and the solution was purged with hydrogen gas.

from that of the fresh steel. Also noted is that the broad current peak at approximately 0.7 V with fresh AISI446 seems shifting cathodically to 0.5–0.55 V. Overall, compared to the fresh steel, the current densities of the 2 h nitrided AISI446 are reduced over the potential range of interest, indicating a moderate improvement in the corrosion resistance resulting from thermal nitridation.

Potentiostatic polarization measurements for 2 h nitrided AISI446 in 1 M H_2SO_4 + 2 ppm F^- at 70 °C are shown in Fig. 4 for 0.6 V in air-sparged solution (cathodic simulation, Fig. 4a) and −0.1 V in hydrogen sparged solution (anodic simulation, Fig. 4b). In the simulated cathodic environment, the corrosion current density quickly stabilized to about 0.6×10^{-6} A cm^{-2}. The corrosion current density stabilized on the order of -1×10^{-6} A cm^{-2} under the simulated anodic conditions, with the sign of the current suggesting protection rather than anodic dissolution. These current densities were comparable to the untreated AISI446 in this environment,

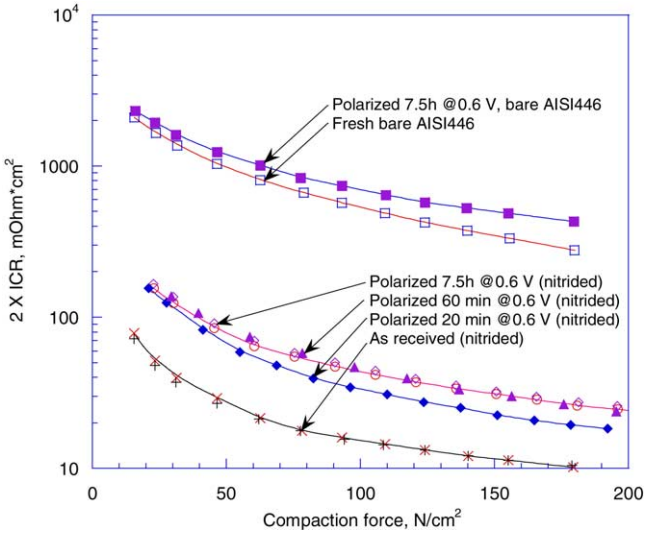

Fig. 5. Comparison of the influence of polarization in simulated PEMFC cathode environment on the ICRs of nitrided and un-nitrided 446. Note that the *y*-axis uses two times of ICR meaning that two interfaces are plotted altogether.

and are sufficiently low to indicate promise for PEMFC applications.

A significant, and highly beneficial effect of the 2 h nitridation became apparent on examination of ICR (Fig. 5). Nitridation decreased the ICR of AISI446 stainless steel by well over an order of magnitude. The effect was particularly evident at the low loads relevant to fuel cell stacks, in the range of 100–150 N cm^{-2}. Polarization under simulated cathodic conditions did raise the ICR of the 2 h nitrided AISI446 stainless steel, which increased with time for the first hour of polarization in the air purged solution at 0.6 V, and then reached a limiting value between 1 and 7.5 h of polarization time. Similar behavior trends of reaching a limiting value of ICR with a polarization time between 1 and 7.5 h was also observed for untreated 349^{TM} stainless steel alloy under these same test conditions [8]. However, the magnitude of the increased ICR for the nitrided AISI446 with polarization was small, with the ICR levels remaining below 40×10^{-3} Ω cm^2 at a load of 150 N cm^{-2}. Therefore, the 2 h 1100 °C nitridation treatment for AISI446 stainless steel modified the surface such that the ICR was significantly decreased, and further, moderately improved on the already promising corrosion resistance of untreated AISI446 under the simulated PEMFC test conditions examined.

Microstructural examination revealed that the 2 h nitridation treatment yielded a different microstructure than either that produced by the 24 h treatment (Fig. 2) or was observed in the nitrided Ni–50Cr model alloy [5]. SEM cross-section analysis (Fig. 6) shows no evidence of a significant Cr-nitride surface layer and reveals only a minor amount of near-surface internal nitride precipitates. Glancing angle XRD (Fig. 7) indicates the presence primarily of ferrite, with minor amounts of $(Cr,Fe)_2N_{1-x}$ (x = 0–0.5) and CrN. Cross-section TEM

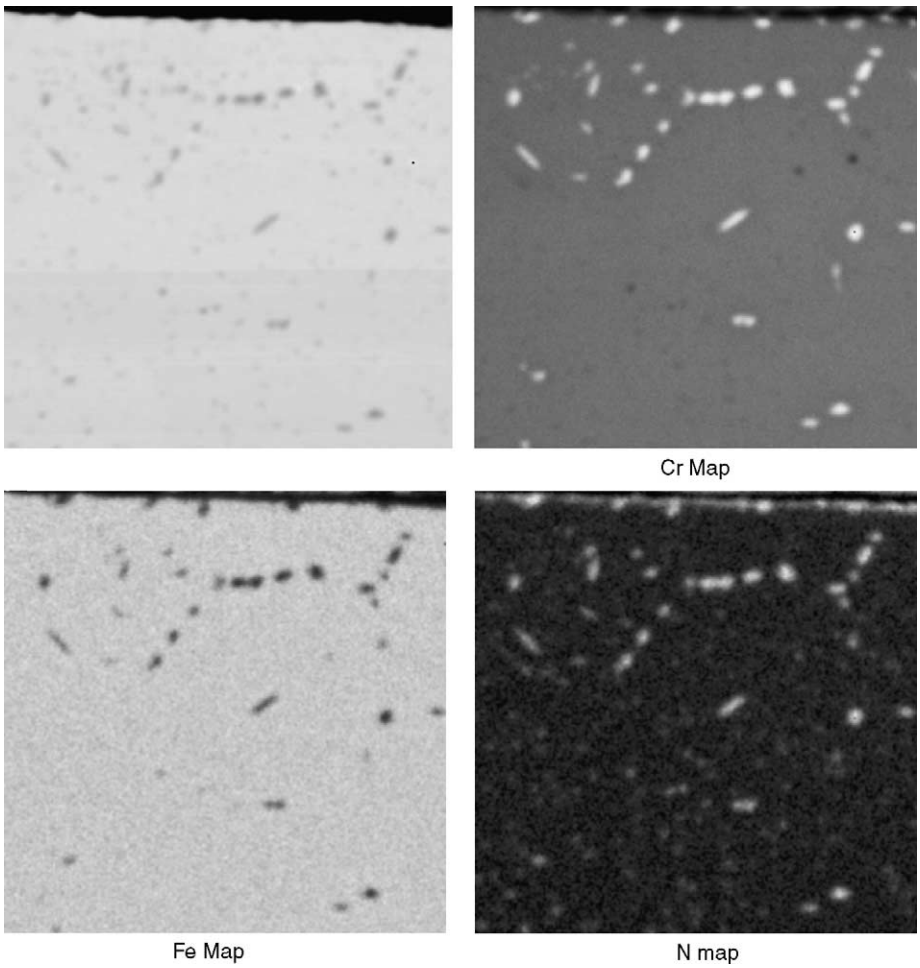

Fig. 6. SEM cross-section and elements mapping of 2 h nitrided AISI446 steel.

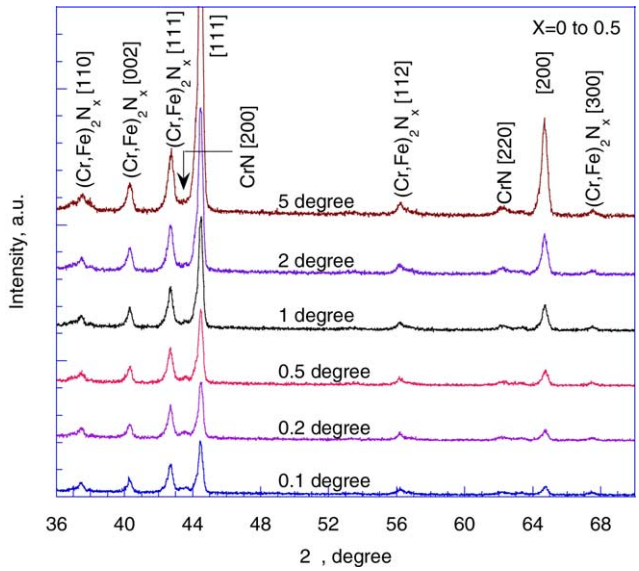

Fig. 7. Glancing angle XRD pattern for 2 h thermally nitrided AISI446 stainless steel.

(Fig. 8) reveals isolated, inward-growing surface grains on the order of 1 μm deep, consistent with Cr_2N (or $(Cr,Fe)_2N_{1-x}$), and patches of a possibly semi-continuous surface layer over both Cr-nitride and ferrite regions on the order of 100 nm thick, which appeared to consist of distinct Al-oxide and Ti-nitride particles. XPS analysis (Fig. 9) is consistent with the microstructures observed in TEM, and suggested a near-surface region rich in Cr-nitrides, Ti-nitrides, Al-oxides, Fe metal and Cr metal. It is particularly interesting to note that the levels of oxygen detected at the surface were significantly higher than the levels of nitrogen. Preliminary, more detailed analysis by Auger suggested a very complex, chemically heterogeneous surface (with many alloy elements and impurities detected) rather than a uniform or semi-uniform surface layer exclusively rich in Al, Ti, or Cr (further studies of this surface are planned).

The data suggest that the 1100 °C 2 h nitridation treatment for AISI446 resulted in a nitrogen modification of the native passive oxide layer on the alloy, which improved corrosion resistance in the aggressive simulated PEMFC anode and cathode environments, and significantly decreased ICR. Further, this surface modification proved resistant to significant

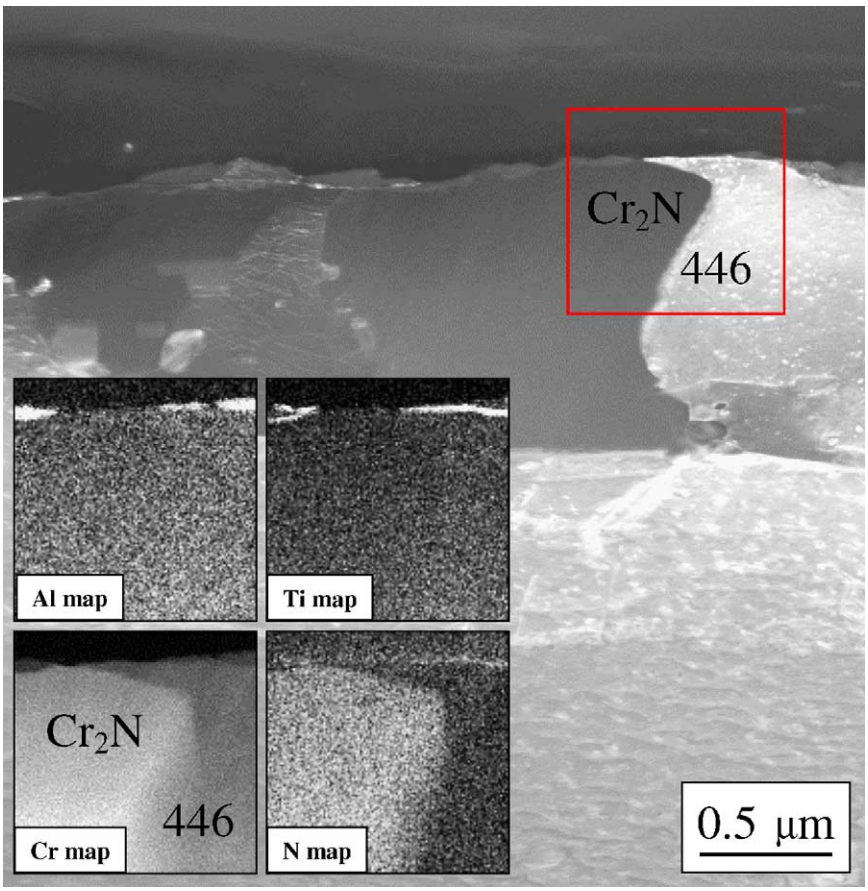

Fig. 8. TEM cross-section of the 2 h nitrided AISI446 steel and the elements mapping.

ICR increase with polarization under passivating conditions. This is an entirely different surface modification phenomenon and effect than that observed for the nitriding of the model Ni–50Cr alloy, which resulted in a microns-thick exclusive and protective Cr-nitride surface layer [2,5].

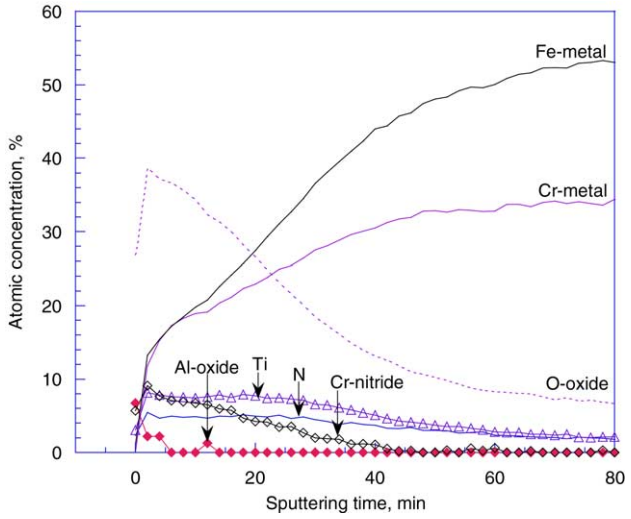

Fig. 9. XPS depth profile of 2 h nitrided AISI446 stainless steel.

4. Concluding remarks

At this stage, it is not clear what aspects of the nitrogen modified surface are specifically responsible for the low ICR and good corrosion resistance of the 2 h nitrided AISI446 or whether such effects can be induced in other stainless steel alloys through proper selection of nitridation conditions. A key aspect is likely the relatively high Cr content of the 446 stainless steel, which was sufficiently high to limit the extent to which Fe was involved in the nitriding reaction at 1100 °C for 2 h in pure nitrogen, compared with the 349^{TM} stainless steel, but not sufficiently high that the desired continuous inward growing Cr-nitride layer was formed, as was observed for Ni–50Cr. In comparison with 349^{TM}, the importance of the austenitic versus ferritic structure is not yet clear, nor is the role of alloy impurities such as Ti and Al, which were observed to segregate to the surface in AISI446. It is possible that selection of less reactive nitriding conditions for 349^{TM} (lower temperature/shorter time) could result in a similar nitrogen-modified passive layer and associated promising corrosion and ICR properties. It may also be possible that the Ti and Al content, or other microalloying additions, are the key to this effect. Further work is planned to sort out these issues. It is also not yet clear if the nitrogen modified passive

layer formed on the 2 h nitrided AISI446 will translate into promising fuel cell performance; however, the formation of an inward-growing $(Cr,Fe)_2N_{1-x}$ layer on 24 h nitrided 446, although not continuous, bodes well for further modification of this class of alloys/nitridation conditions to achieve a continuous protective layer, analogous to the Cr-nitrides on Ni–50Cr. Fuel cell test evaluation of bipolar plates of AISI446 nitrided in this manner is planned.

Acknowledgement

The authors wish to thank Dr. Glenn Teeter for helping the AES measurements. This work was supported by the Hydrogen, Fuel Cell and Infrastructure Technologies Program of the U.S. Department of Energy. Oak Ridge National Laboratory is managed by UT-Battelle, LLC for the US DOE under contract DE-AC05-00OR22725.

References

[1] B.C.H. Steele, A. Heinzel, Nature (London) 414 (2001) 345.
[2] M.P. Brady, K. Weisbrod, I. Paulauskas, R.A. Buchanan, K.L. More, H. Wang, M. Wilson, F. Garzon, L.R. Walker, Scripta Mater. 50 (2004) 1017.
[3] M.P. Brady, K. Weisbrod, C. Zawodzinski, I. Paulauskas, R.A. Buchanan, L.R. Walker, Electrochem. Solid-State Lett. 5 (2002) 245–247.
[4] M.P. Brady, I. Paulauskas, R.A. Buchanan, K. Weisbrod, H. Wang, L.R. Walker, L.S. Miller, Proceedings of the 2nd European PEFC Forum, Lucerne, Switzerland, 30 June, 2003.
[5] H. Wang, M.P. Brady, J.A. Turner, Thermally nitrided stainless steels for PEMFC bipolar plates. Part 1: Model Ni–50Cr and austenitic 349TM alloys, J. Power Sources, in press.
[6] H. Wang, J.A. Turner, J. Power Sources 128 (2004) 193.
[7] H. Wang, M.A. Sweikart, J.A. Turner, J. Power Sources 115 (2) (2003) 243.
[8] H. Wang, G. Teeter, C. Jiang, J.A. Turner, On the passivation of 349^{TM} stainless steel in a simulated PEMFC cathode environment, Corros. Sci., in press.